

$^{14}\text{Be}(p, n)^{14}\text{B}$ reaction at 69 MeV in inverse kinematics

Y. Satou,^{1,*} T. Nakamura,² Y. Kondo,² N. Matsui,² Y. Hashimoto,² T. Nakabayashi,²
T. Okumura,² M. Shinohara,² N. Fukuda,³ T. Sugimoto,³ H. Otsu,³ Y. Togano,³ T. Motobayashi,³
H. Sakurai,³ Y. Yanagisawa,³ N. Aoi,³ S. Takeuchi,³ T. Gomi,³ M. Ishihara,³ S. Kawai,⁴ H.J. Ong,⁵
T.K. Onishi,⁵ S. Shimoura,⁶ M. Tamaki,⁶ T. Kobayashi,⁷ Y. Matsuda,⁷ N. Endo,⁷ and M. Kitayama⁷

¹*Department of Physics and Astronomy, Seoul National University, 599 Gwanak, Seoul 151-742, Korea*

²*Department of Physics, Tokyo Institute of Technology,
2-12-1 Oh-Okayama, Meguro, Tokyo 152-8551, Japan*

³*RIKEN Nishina Center, 2-1 Hirosawa, Wako, Saitama 351-0198, Japan*

⁴*Department of Physics, Rikkyo University, 3 Nishi-Ikebukuro, Toshima, Tokyo 171-8501, Japan*

⁵*Department of Physics, University of Tokyo, 7-3-1 Hongo, Bunkyo, Tokyo 113-0033, Japan*

⁶*Center for Nuclear Study (CNS), University of Tokyo, 2-1 Hirosawa, Wako, Saitama 351-0198, Japan*

⁷*Department of Physics, Tohoku University, Aoba, Sendai, Miyagi 980-8578, Japan*

(Dated: May 28, 2019)

A Gamow-Teller (GT) transition from the drip-line nucleus ^{14}Be to ^{14}B was studied via the (p, n) reaction in inverse kinematics using a secondary ^{14}Be beam at 69 MeV/nucleon. The invariant mass method is employed to reconstruct the energy spectrum. A peak is observed at an excitation energy of 1.27(2) MeV in ^{14}B , together with bumps at 2.08 and 4.06(5) MeV. The observed forward peaking of the state at 1.27 MeV and a good description for the differential cross section obtained with a DWBA calculation provide support for the 1^+ assignment to this state. By extrapolating the cross section to zero momentum transfer the GT-transition strength is deduced. The value is found to compare well with that reported in a β -delayed neutron emission study.

Keywords: Gamow-Teller transition, $^1\text{H}(^{14}\text{Be}, ^{13}\text{B}+n)$, Unbound states, Distorted-wave approximation

The Gamow-Teller (GT) transition, characterized by an angular momentum transfer of $\Delta L=0$, a spin transfer of $\Delta S=1$, and an isospin transfer of $\Delta T=1$ between initial and final nuclei, represents one of the fundamental modes of nuclear excitations. Its properties are important not only for understanding spin-isospin correlations in nuclei [1], but also for their implications for a variety of astrophysical phenomena where weak processes play a key role, such as late stages of stellar evolution and neutrino nucleosynthesis [2]. The rapid increase in the availability of Radioactive Isotope (RI) beams in recent years has made it possible to study GT strengths in nuclei far from the β -stability line. Although β decay has been the major source of information about such strengths, it might be expected that nuclear charge-exchange (CE) reactions play an important role [3], with their distinguishing feature of being unconstrained by any Q_β limitations. We performed an experimental study of the (p, n) reaction on a neutron-rich nucleus ^{14}Be using the invariant mass method in inverse kinematics. The data on the $^{14}\text{Be}(\text{g.s.}) \rightarrow ^{14}\text{B}(1_1^+)$ transition process enables the extraction of $B(\text{GT})$ from forward angle (p, n) cross sections. Studies were also made on states populated in the $^1\text{H}(^{14}\text{Be}, ^{13}\text{B}+n)$ reaction.

The ^{14}Be nucleus is located at the neutron drip line. A two-neutron halo structure has been suggested by inclusive [4, 5] as well as exclusive [6] reaction studies. Unambiguous identification of the first 2^+ state was made recently [7]. The β decay of ^{14}Be is known to be dominated by one-neutron emission with a branching ratio compatible with 100% [8]. A concentration of the decay

strength in a state at 1.28 MeV, which is located just above the one-neutron separation energy of $S_n=0.97(2)$ MeV [11] in ^{14}B , was found in energy spectra of decay neutrons [9, 10]. The small $\log ft$ value of 3.68(5) [10] has indicated that the decay is due to a GT transition, providing the 1^+ assignment to this state.

Existing CE studies on β -unstable nuclei have been based on two major methods: the first involves final states in a bound region and the missing mass technique was applied, where momenta of heavy charged ejectile were measured either by using a spectrograph in the $^6\text{He}(p, n)^6\text{Li}$ [12, 13] and $^{34}\text{P}(^7\text{Li}, ^7\text{Be} + \gamma)^{34}\text{Si}$ [14] reactions, or a telescope in the $^6\text{He}(p, n)^6\text{Li}$ reaction [15]. The second method involves unbound final states, and the invariant mass technique was adopted. All particles from a decay of an unbound state were detected using a plastic counter hodoscope in the $^{11}\text{Li}(p, n)^{11}\text{Be}$ [16] and $^{14}\text{Be}(p, n)^{14}\text{B}$ [17] reactions; isobaric analog states in the residual nuclei were identified. Until now, there exist only a limited number of CE studies involving unstable nuclear beams; it is desirable to further explore experimental approaches which permit reliable determination of relevant nuclear structure information. The present study, succeeding to the latter works, represents the first extraction of the GT strength on an unstable nucleus, leading to a particle unbound state in an inverse kinematics CE reaction. Independent detectors were used for different decay products, charged fragment and neutron, to achieve high enough acceptance near the threshold, together with a liquid hydrogen target to increase the reaction yield. In inverse kinematics, decay neutrons emit

ted from the unbound system, which is Lorentz boosted with a beam-like velocity in the laboratory, acquire high energies and can be detected with high efficiencies. With this new feature, it is shown that the inverse kinematics CE reaction accompanied by neutron decay provides an alternative approach for nuclear structure, to β -delayed neutron spectroscopy.

The extraction of the GT strength in CE reactions relies on the proportionality relationship between the reduced transition probability $B(\text{GT})$ and the cross section at zero momentum transfer ($q=0$) [18, 19]:

$$(d\sigma/d\Omega)_{q=0}^{L=0} = \left[\frac{E_i E_f}{(\hbar^2 c^2 \pi)^2} \right] N_D |J_{\sigma\tau}|^2 B(\text{GT}). \quad (1)$$

Here $E_{i(f)}$ is the reduced energy in the initial (final) channel and $|J_{\sigma\tau}|$ is the volume integral of the central part of the effective nucleon-nucleon (NN) interaction in the spin-isospin channel. The distortion factor $N_D = (d\sigma/d\Omega)_{q=0}^{\text{DW}} / (d\sigma/d\Omega)_{q=0}^{\text{PW}}$ is the ratio of distorted-wave (DW) and plane-wave (PW) cross sections. The cross section $(d\sigma/d\Omega)_{q=0}^{L=0}$, defining the $L=0$ contribution at $q=0$, is obtained by extrapolating the 0° cross section to $q=0$ using the ratio of distorted-wave Born approximation (DWBA) cross sections at $q=0$ and 0° , with an additional factor given by the ratio of the cross section calculated with only the central terms of the NN interaction and that with the full force components. Although the above relationship [Eq.(1)] has been mainly used for CE reaction data at bombarding energies above 100 MeV/nucleon, it is expected to be applicable for (p, n) scattering data involving transitions with appreciable strengths, at energies of the present work (around $E_p=70$ MeV), due to the simple reaction mechanism of the nucleon scattering and to the availability of modern nucleon-nucleus optical model potentials (OMPs).

The experiment was performed at the projectile-fragment separator RIPS [20], which is a part of the RIBF accelerator complex operated by RIKEN Nishina Center. The setup was identical to the one used in Ref. [21]. The radioactive beam of ^{14}Be was produced from a 100-MeV/nucleon ^{18}O beam, which impinged on a 6-mm-thick Be target. The typical beam intensity was 7 kcps with a momentum spread of $\Delta P/P = \pm 2\%$. The beam profile was monitored by two sets of parallel-plate avalanche counter (PPAC), placed upstream of the target. The secondary target was a liquid hydrogen target [22] with a cylindrical shape: 3 cm in diameter and 229 ± 6 mg/cm² in thickness. The average energy of ^{14}Be at the target center was 69 MeV/nucleon. The target was surrounded by a NaI(Tl) scintillator array to detect γ rays from charged fragments. The fragments bent by a dipole magnet behind the target were detected by a plastic counter hodoscope, which gave Z identification by ΔE . Their trajectory was measured by a set of multi-wire drift chambers placed before and after the magnet,

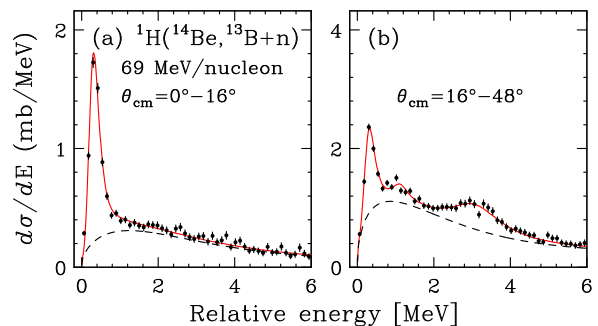


FIG. 1. Relative energy spectra of the $^1\text{H}(^{14}\text{Be}, ^{13}\text{B} + n)$ reaction for (a) $\theta_{\text{cm}}=0^\circ-16^\circ$ and (b) $\theta_{\text{cm}}=16^\circ-48^\circ$.

which, together with time of flight, gave mass identification. Neutrons were detected by two walls of plastic scintillator arrays placed 4.6 and 5.8 m downstream of the target. The neutron detection efficiency was $24.1 \pm 0.8\%$ for a threshold setting of 4 MeVee. The relative energy E_{rel} of the final system was calculated from the momentum vectors of the charged fragment and the neutron. The bending magnet for the fragment allowed the two detector systems to be located separately. This, together with the kinematical focusing of the reaction products toward forward angles, ensured that the phase space volume of the final decaying system was covered efficiently.

Figure 1 shows relative energy spectra obtained at two different angular bins: (a) $\theta_{\text{cm}}=0^\circ-16^\circ$ and (b) $\theta_{\text{cm}}=16^\circ-48^\circ$. The effects of finite detector acceptances were corrected. Background contributions due to window materials, measured with an empty target, were less than 0.1 mb/MeV, and were subtracted in the figure. Error bars are statistical ones. A sharp resonance peak, evident at $E_{\text{rel}} \approx 0.3$ MeV, is most prominent at forward angles. A bump structure at $E_{\text{rel}} \approx 1.1$ MeV is visible only at backward angles, and might correspond to the reported 4^- , 2.08 MeV state observed in the $^{14}\text{C}(^7\text{Li}, ^7\text{Be})^{14}\text{B}$ [23] and $^{12}\text{C}(^{14}\text{C}, ^{12}\text{N})^{14}\text{B}$ [24] reactions. Since this state is weakly populated, the energy of 2.08 MeV was adopted in the subsequent analysis. Another bump at $E_{\text{rel}} \approx 3$ MeV was observed for the first time in this study. For the three states no coincident γ rays were identified.

The spectra were analyzed using single Breit-Wigner shape functions as described in Ref. [25] to extract the resonance energy E_r , width Γ_r , and peak yield. The line shape was obtained in a Monte Carlo simulation which includes the detector response, beam profile, and target thickness. The relative energy resolution was well described by the relationship: $\Delta E_{\text{rel}} = 0.20\sqrt{E_{\text{rel}}}$ MeV(rms). For strengths beneath the resonance, thermal emission of a neutron from the continuum [26] was assumed. A constant background, which simulates various effects such as overlapping broad resonances and decay to an excited residue was also introduced when needed. Solid lines in Fig. 1 are the results of the fit; the assumed continuum-

TABLE I. Resonance parameters in the present analysis. The excitation energy of $E_x=2.08$ MeV is from Refs. [23, 24].

E_r (MeV)	E_x (MeV)	Γ_r (MeV)	l (\hbar)	J^π
0.304(4)	1.27(2)	0.16(2)	1	1^+
1.11	2.08	—	2	4^-
3.09(5)	4.06(5)	[1.0(3),1.2(5)]	(1,2)	($3^+,3^-$)

like strengths are indicated as dashed lines. Resulting resonance parameters are summarized in Table I. The orbital angular momenta (l) of decay neutrons are also shown. The excitation energy ($E_x=E_r+S_n$) of 1.27(2) MeV for the peak at $E_{\text{rel}}\approx 0.3$ MeV agrees well with the reported value of 1.28(2) MeV for the first 1^+ state in ^{14}B [9, 10]. The width of $\Gamma_r=0.16(2)$ MeV is consistent with the single-particle estimate of $\Gamma_{\text{sp}}=0.31$ MeV for an $l=1$ resonance calculated in a Woods-Saxon potential, while it is significantly larger than $\Gamma_{\text{sp}}=0.02$ MeV for a d -wave, supporting the assumption of a p -wave decay. It is to be noted that the single particle width, Γ_{sp} , is an estimate of the total decay width derived within the one-particle model in a simple nuclear potential, and that it provides an upper limit for the actual nucleus case where the configuration mixing is generally important. For the 2.08 MeV state, the width was not reliably extracted due to limited signal-to-background ratio near the resonance; it was assumed to be dominated by the resolution. Note that an experimental upper limit of $\Gamma_r=0.1$ MeV [24] has been reported. For the 4.06 MeV state two different decay angular momenta, $l=1$ and 2, were considered. The deduced widths are shown in Table I. The resonance energy was similar in the two cases and varied within the errors.

Figure 2 shows differential cross sections leading to the observed states. These were obtained by subdividing the acceptance solid angle to have a spectrum at each angular bin, and applying the fitting procedure to extract the peak yields. Error bars are statistical ones; systematic uncertainties are estimated to be 6%, including those in the target thickness, neutron detection efficiency, and fitting procedure. The resolution in the scattering angle was estimated with the Monte Carlo simulation to vary from $\Delta\theta_{\text{cm}}=2.3^\circ$ in rms at $\theta_{\text{cm}}=4^\circ$ to 4.5° at $\theta_{\text{cm}}=44^\circ$.

Microscopic DWBA calculations were performed to clarify the nature of states observed and to have a means to extrapolate the 1^+ cross section to $q=0$. The OMP was taken from the semi-microscopic parametrization of JLMB [28]. Within the local density approximation, the local value of the finite nucleus OMP was deduced from the nuclear matter OMP. The proton and neutron radial density distributions were calculated in a mean field using the SkX interaction [29]. The effective NN interaction was the M3Y interaction [30] (force components labeled 1,4,11,14,16,17, and 20 were used). The transition density was obtained from the shell model using the code

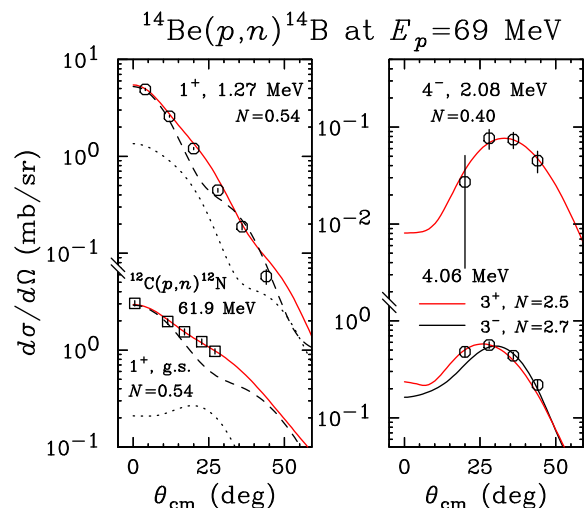


FIG. 2. Angular distributions of the differential cross section leading to the three states observed (open circles). Data for the $^{12}\text{C}(p,n)^{12}\text{N}(1^+, \text{g.s.})$ reaction at 61.9 MeV [27] (open squares) are also shown. Normalization factors applied to the DWBA curves (solid lines) are indicated in the figure. Additional curves, dashed and dotted lines, given for $0^+ \rightarrow 1^+$ transitions are DWBA results obtained, respectively, with only the central and tensor terms of the NN interaction.

OXBASH [31]. The calculations used the WBT Hamiltonian [32] in the $spsdpf$ model space within the $0\hbar\omega$ configuration. The single-particle wave functions were generated in a harmonic oscillator well with an oscillator parameter $b=2.04(6)$ fm, chosen to reproduce the rms matter radius of ^{14}Be [33]. The code DW81 [34] was used for the calculations.

The DWBA cross sections are shown as solid lines in Fig. 2. Normalization factors required for the theoretical curves to reproduce the data are also indicated. For the calculation of the 1.27 MeV state, the wave function of the first 1^+ shell-model state predicted at 1.01 MeV was used, while for the 2.08 MeV state that of the first 4^- state at 1.75 MeV was used. The measured cross sections leading to these states, which exhibit characteristic angular distribution patterns, are well reproduced by the calculations, corroborating the earlier spin-parity (J^π) assignments of 1^+ for the 1.27 MeV state [10] and 4^- for the 2.08 MeV state [23, 24]. For the 4.06 MeV state, the calculation was repeated by assuming different shell-model wave functions with various J^π values. The angular distribution was found to be best described by the curve assuming the second 3^+ state predicted at 4.20 MeV (red line). Another possible candidate was the second 3^- state at 5.70 MeV. Although the calculated cross section, shown in Fig. 2 as a black line, is slightly backward peaked, it is compatible with the data and the possibility could not be completely ruled out. With this a tentative J^π assignment of 3^+ or 3^- is made to this state. It would be interesting if we could distinguish the

two cases by experiments with different sensitivity from the present one.

The extraction of $B(\text{GT})$ leading to the 1^+ , 1.27 MeV state was done by using Eq.(1). The DWBA framework as described above was utilized to calculate the parameter for momentum extrapolation and the distortion factor. In order to see the contribution from the non-central terms of the NN interaction, two kinds of additional DWBA calculations were performed: one with only the central terms and the other with only the tensor terms, and the results of these calculations are shown as dashed and dotted lines in Fig. 2, respectively (the contribution from the spin-orbit terms turned out to be negligibly small). The ratio of the cross section calculated with only the central terms to that with full force components was 0.961 at $\theta=0^\circ$, while it was closer to unity, 1.008, at $q=0$. Two additional sets of OMP parameters [35, 36] were used to estimate the uncertainty due to the choice of the optical model. For calculations of the cross section at $q=0$, the distorting potential in the exit channel was re-evaluated at a neutron energy which satisfies the kinematical constraint. The volume integral $|J_{\sigma\tau}|$ of the NN interaction can be deduced effectively by analyzing the existing $(p, n) 0^+ \rightarrow 1^+$ transition data at a similar incident energy, for which the $B(\text{GT})$ value is well established. The $^{12}\text{C}(p, n)^{12}\text{N}(1^+, \text{g.s.})$ reaction data at 61.9 MeV [27], with the corresponding $B(\text{GT})$ value of 0.875(6) [37], were used for this purpose. In the DWBA analysis, three sets of OMP parameters [28, 35, 36] and the P(10–16)T shell-model wave function [32] were used. The oscillator parameter chosen was $b=1.87$ fm [38], which reproduces the maxima of the electron scattering form factors. A result of the fit of the theoretical curve, calculated with the JLMB [28] OMP, to the data is shown as a solid line in Fig. 2. Dashed and dotted curves are again DWBA cross sections calculated with only the central and tensor terms of the NN interaction, respectively. For this transition, switching off the tensor terms had an effect to reduce the cross section by 1.3% (–0.8%) at $\theta=0^\circ$ ($q=0$). By using Eq.(1), $|J_{\sigma\tau}|$ at 61.9 MeV was deduced to be $212.1 \pm 3.1(\text{stat}) \pm 9.3(\text{syst})$ MeV fm³, where the systematic error includes the uncertainty due to the choice of optical parameters (2%). The value turns out to be consistent with the tabulated ones for the M3Y interaction [39]: $|J_{\sigma\tau}|=211(247)$ MeV fm³ at $E_p=61(40)$ MeV. From the proportionality between the cross section at $q=0$ and $B(\text{GT})$ [Eq.(1)], which assumes $|J_{\sigma\tau}|$ at 69 MeV obtained by making energy extrapolation using values for the M3Y interaction, the $B(\text{GT})$ for the transition to the 1^+ state at 1.27 MeV in ^{14}B was found to be $0.79 \pm 0.03(\text{stat}) \pm 0.09(\text{syst})$. The systematic error includes the uncertainty due to the choice of optical parameters (4%). The value is in good agreement with the β -decay value of $B(\text{GT})=0.80 \pm 0.09$ [10], calculated from the ft value using the relationship: $B(\text{GT})=(g_A/g_V)^{-2}(6147/ft)$ [1].

The shell-model prediction obtained using the WBT interaction [32] and the effective GT operators [40], within the $0\hbar\omega$ basis, is $B(\text{GT})=0.88$, which is consistent with the data. This suggests that the ground state of ^{14}Be is predominantly of $0\hbar\omega$ nature. Precision data and improved knowledge on effective GT operators will allow further detailed analyses of the admixtures of higher- $\hbar\omega$ intruder components [41], in terms of $B(\text{GT})$.

The $^{14}\text{Be}(\text{g.s.}) \rightarrow ^{14}\text{B}(1_1^+)$ transition exhausts only a minor fraction ($\sim 4\%$) of the GT sum rule: $3(N-Z)=18$. Major GT strengths are expected to be located at previously unexplored high excitation energy regions [42, 43]. CE studies probing such strengths are a challenge (this might need either multiple-neutron detection within the current invariant mass scheme or recoiled-neutron detection in the missing mass scheme), but will shed new light on our understanding of spin-isospin correlations in nuclei at extreme conditions of isospin and binding energy. The present study, quantifying the accuracy for a procedure to extract $B(\text{GT})$ from forward angle (p, n) cross sections on radioactive beams to be of order 15%, paves the way for future investigations in this direction.

In summary, the (p, n) reaction on ^{14}Be was measured at 69 MeV/nucleon using the invariant mass method. In decay energy spectra three resonance states were observed. A comparison of measured cross sections with DWBA calculations yielded a confirmation of the earlier J^π assignments of 1^+ and 4^- for the 1.27 and 2.08 MeV states, respectively. It also led to a tentative J^π assignment of 3^+ or 3^- for a state newly observed at 4.06 MeV. By extrapolating the cross section to $q=0$, the $B(\text{GT})$ leading to the 1^+ state was deduced, which compares well with the β -decay value, providing the first successful demonstration of an experimental capability of extracting GT strengths on unstable nuclei via decay spectroscopy following CE reactions in inverse kinematics.

The authors are grateful for the invaluable assistance of the staff of RIKEN during the experiment. They thank Professor J.A. Tostevin for reading the manuscript. The work was in part supported by the Grant-in-Aid for Scientific Research (No. 15740145) of MEXT Japan and the WCU program (R32-2008-000-10155-0) of NRF Korea.

* satou@smu.ac.kr

- [1] M.N. Harakeh, A. van der Woude, *Giant Resonances* Oxford University Press, New York, 2001).
- [2] K. Langanke, G. Martínez-Pinedo, *Rev. Mod. Phys.* 75 (2003) 819.
- [3] S.M. Austin, in *Proc. Int. Symp. on New Facet of Spin Giant Resonances in Nuclei*, edited by H. Sakai, et al. (World Scientific, Singapore, 1998), p.347.
- [4] I. Tanihata, et al., *Phys. Lett. B* 206 (1988) 592.
- [5] M. Zahar, et al., *Phys. Rev. C* 48 (1993) R1484.

- [6] M. Labiche, et al., Phys. Rev. Lett. 86 (2001) 600.
- [7] T. Sugimoto, et al., Phys. Lett. B 654 (2007) 160.
- [8] U.C. Bergmann, et al., Nucl. Phys. A 658 (1999) 129.
- [9] M. Belbot, et al., Phys. Rev. C 56 (1997) 3038.
- [10] N. Aoi, et al., Phys. Rev. C 66 (2002) 4301.
- [11] G. Audi, et al., Nucl. Phys. A 729 (2003) 337.
- [12] J.A. Brown, et al., Phys. Rev. C 54 (1996) R2105.
- [13] M.D. Cortina-Gil, et al., Phys. Lett. B 371 (1996) 14.
- [14] R.G.T. Zegers, et al., Phys. Rev. Lett. 104 (2010) 212504.
- [15] Z. Li, et al., Phys. Lett. B 527 (2002) 50.
- [16] T. Teranishi, et al., Phys. Lett. B 407 (1997) 110.
- [17] S. Takeuchi, et al., Phys. Lett. B 515 (2001) 255.
- [18] C.D. Goodman, et al., Phys. Rev. Lett. 44 (1980) 1755.
- [19] T.N. Taddeucci, et al., Nucl. Phys. A 469 (1987) 125.
- [20] T. Kubo, et al., Nucl. Instrum. Methods Phys. Res. Sect. B 70 (1992) 309.
- [21] Y. Kondo, et al., Phys. Lett. B 690 (2010) 245.
- [22] H. Ryuto, et al., Nucl. Instrum. Methods Phys. Res. Sect. A 555 (2005) 1.
- [23] G.C. Ball, et al., Phys. Rev. Lett. 31 (1973) 395.
- [24] R. Kalpakchieva, et al., Eur. Phys. J. A 7 (2000) 451.
- [25] Y. Satou, et al., Phys. Lett. B 660 (2008) 320.
- [26] F. Deák, et al., Nucl. Instrum. Methods Phys. Res. Sect. A 258 (1987) 67.
- [27] B.D. Anderson, et al., Nucl. Instrum. Methods 169 (1980) 153.
- [28] E. Bauge, J.P. Delaroche, M. Girod, Phys. Rev. C 63 (2001) 024607.
- [29] B.A. Brown, Phys. Rev. C 58 (1998) 220.
- [30] G. Bertsch, et al., Nucl. Phys. A 284 (1977) 399.
- [31] B.A. Brown, et al., NSCL Report No. MSUCL-1289.
- [32] E.K. Warburton, B.A. Brown, Phys. Rev. C 46 (1992) 923.
- [33] A. Ozawa, T. Suzuki, I. Tanihata, Nucl. Phys. A 693 (2001) 32.
- [34] R. Schaeffer, J. Raynal, DWBA70 (unpublished), Extended version DW81, J.R. Comfort (unpublished).
- [35] R.L. Varner, et al., Phys. Rep. 201 (1991) 57.
- [36] A.J. Koning, J.P. Delaroche, Nucl. Phys. A 713 (2003) 231.
- [37] F. Ajzenberg-Selove, Nucl. Phys. A 506 (1990) 1.
- [38] J.R. Comfort, et al., Phys. Rev. C 24 (1981) 1834.
- [39] W.G. Love, in *The (p,n) Reaction and the Nucleon-Nucleon Force*, edited by C.D. Goodman, et al. (Plenum, New York, 1980), p.23.
- [40] W.-T. Chou, E.K. Warburton, B.A. Brown, Phys. Rev. C 47 (1993) 163.
- [41] A. Umeya, G. Kaneko, T. Haneda, K. Muto, Phys. Rev. C 77 (2008) 044301.
- [42] H. Sagawa, I. Hamamoto, M. Ishihara, Phys. Lett. B 303 (1993) 215.
- [43] T. Suzuki, T. Otsuka, Phys. Rev. C 56 (1997) 847.